GHGSat Constellation: The Future of Monitoring Greenhouse Gas Emissions

Michael Ligori, Laura Bradbury, Robert Spina, Robert E. Zee
Space Flight Laboratory, University of Toronto Institute for Aerospace Studies
4925 Dufferin Street, Toronto, ON, Canada, M3H 5T6; +1 416 667 7498
mligori@utias-sfl.net

Stephane Germain
GHGSat Inc
3981 St-Laurent, Suite 500, Montreal, QC, Canada, H2W 1Y5; 514-874-9474
stephane.germain@ghgsat.com

ABSTRACT

As the effects of greenhouse gas (GHG) and issues resulting from air quality (AQG) become more prevalent, there is increasing motivation for industrial operators to quantify and ultimately reduce their emission footprint. GHGSat Inc., utilizing novel satellite technology developed in partnership with the Space Flight Laboratory, intends to become the global leader of remote sensing of GHG, AQG, and other trace gas emissions. Phase one: GHGSat-D (Claire) launched in June 2016, becoming the first microsatellite with a high-resolution instrument designed to measure greenhouse gas emissions from point sources. With over 3000 site measurements made worldwide, GHGSat-D has proven how effective satellite technology is paving the way forward for a worldwide monitoring initiative: GHGSat Constellation. Phase two: GHGSat-C1 and GHGSat-C2 are in development as first in a fully operational constellation allowing continued enhancement of the satellite design. These enhancements include hardware redundancy and improved electromagnetic compatibility to increase performance and reliability, upgrades to the primary optical payload to reduce the effects of stray light, allow for onboard calibration and improved radiation mitigation, and an optical downlink to increase the downlink capacity of the platform. GHGSat-C1 is scheduled for launch in Q3 2019 with GHGSat-C2 following in 2020.

INTRODUCTION

One of the biggest problems facing the current generation is Earth's changing climate. A key factor in contributing to this problem is the increased concentration of greenhouse gas (GHG) emissions including carbon dioxide (CO_2) and methane (CH_4). CO_2 is the primary GHG emitted as a result of human activities such as burning of fossil fuels and deforestation. Methane is the second highest emission and is produced through activities such as coal mining, landfills and livestock. Around the world, steps are being taken to address climate change from increasing awareness to environmental regulations to national plans aimed at reducing GHG emissions with the ultimate aim of reducing human impact. This task is made all the more difficult as current societal success has been achieved at the cost of harmful emissions and impacts all parts of the economy. The United Nations Framework Convention on Climate Change (UNFCC) annually reports on the estimated CO_2 equivalent emissions in six economic sectors[1]. This is shown in Figure 1.

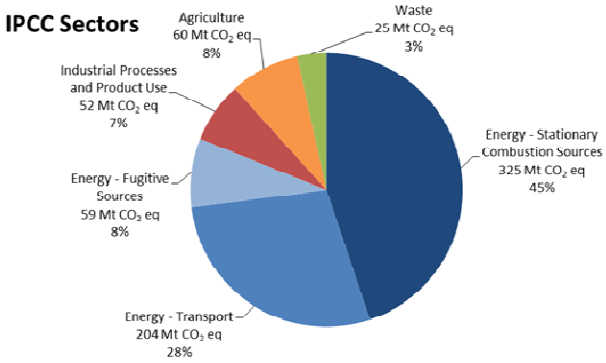

Figure 1: Canada's GHG Emissions by Economic Sector (2015) [1]

As with most problems, having reliable information is often the key to understanding and addressing them however given the spread across industry and the planet itself, traditional approaches of emission measurement are inefficient or ineffective. Global coverage however can be achieved through the use of space based assets. Monitoring time can approach real time scales allowing for instantaneous snapshots of events while revisits of the same area can be used to develop trends. The

usefulness of this approach has previously been demonstrated by such missions as JAXA's Ibuki mission known as Greenhouse gases Observing SATellite (GOSAT). A 1750 kg spacecraft launched in 2009 monitors methane and atmospheric carbon dioxide, with a mission goal to estimate GHG sources and sink on the scale of sub-continents.[2]

GHGSat Inc. of Montréal, Canada intends to become the global leader of remote sensing of GHG, AQG, and other trace gas emissions from any source on the globe by leveraging space assets and utilizing advanced technology. The first step was undertaken with GHGSat-D (Claire), a proof of concept technology demonstrator. It was the first satellite designed to measure point sources of GHG emissions and has collected measurement form over 3000 sites around the world. An example can be seen in Figure 2. This measurement of a hydroelectric dam located in Africa was published in 2017. Not only was Claire a fraction of the size and mass of previous missions, it also boasted an incredible spatial resolution of less than 50 m compared with previous spacecraft which had resolutions on the order of kilometers.

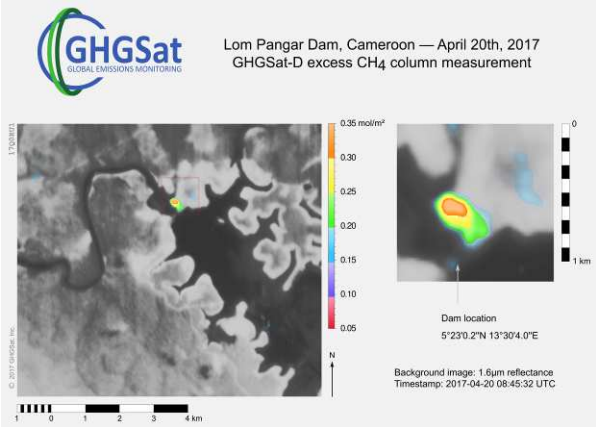

Figure 2: Methane Emissions from the Lom Pangar Dam in Cameroon[3]

GHGSat-D proved that small spacecraft monitoring is possible. It allowed organizations to understand their emission footprint and in the changing climate of carbon tax and carbon pricing, allows them to manage financial risk with the aim of controlling and ultimately reducing emissions. GHGSat-D is just the beginning. It has paved the way forward for a worldwide monitoring initiative: GHGSat Constellation. The next step is GHGSat-C1 and GHGSat-C2 which will employ enhancements learned from GHGSat-D and increase worldwide GHG missions data. GHGSat-C1 is on track for launch in Q3 2019 with GHGSat-C2 following in the first half of 2020.

Figure 3: Artists Rendition of GHGSat-C1/GHGSat-C2 On-Orbit

SATELLITE PLATFORM OVERVIEW

NEMO Platform

GHGSat-D and the upcoming GHGSat-C1/GHGSat-C2 are based off the Next-generation Earth Monitoring and Observation (NEMO) platform, a small SFL microsatellite bus. The bus design consists of two trays enclosed with six panels capable of supporting a maximum payload mass of 6 kg. The bus itself depending on payload and optional SFL avionics can have a mass ranging from 10 to 20 kg. Using GHGSat-D as an example, this structural layout can be seen in Figure 4.

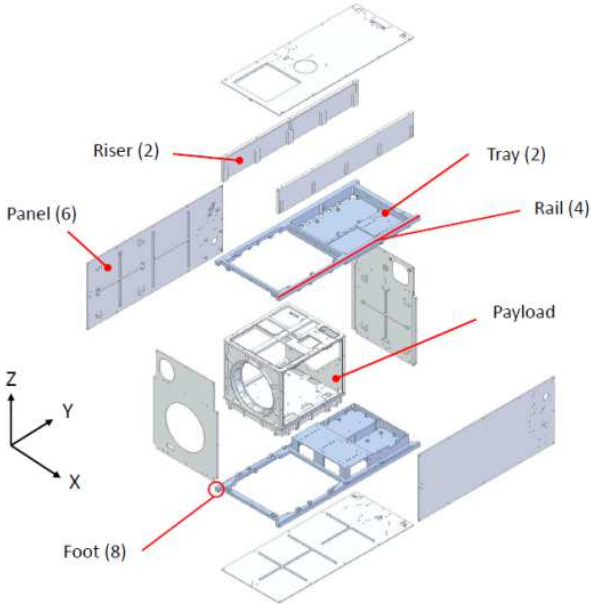

Figure 4: GHGSat-D Structure Exploded View

The nominal spacecraft volume is 20x30x40 cm (not including any pre-deployed appendages) with a nominal payload volume of 8000 cm^3. The peak power of the

bus is 50-100 W with the higher power levels achieved through the use of pre-deployed solar wings. Payload power supports at 40% duty cycle up to 45 W.

Depending on mission goals, a variety of attitude control system (ACS) sensors and actuators can be supported by the NEMO bus. This nominally includes rate sensors, magnetometers, three magnetorquers, three orthogonal reaction wheels and up to six sun sensors. Using this suite of sensors, allows a 2σ pointing accuracy of with ~2° in sunlight and ~5° in eclipse. For those missions that require improved ACS, a star tracker can be included. This increases ACS stability to 10-60 arc seconds. A GPS system can also be included for missions requiring orbital positon and velocity measurements. Example of this ACS package is shown in Figure 5.

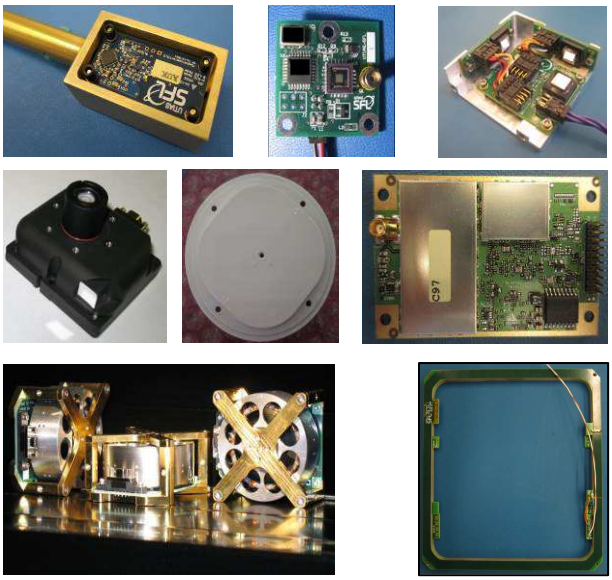

Figure 5: SFL ACS Package

The standard NEMO bus uses S-band downlink and UHF uplink for communications. The downlink, using either BPSK or QPSK modulation, is capable of on-the-fly data rate scaling from 32 kbps to 2048 kbps. The uplink is a fixed 4 kbps data rate. Further options include exchanging the uplink by replacing the UHF uplink with an S-band uplink.

The separation system for the NEMO bus, depending on pre-deployed appendages and protrusions, can either be the XPOD Duo or XPOD Delta. An example is shown in Figure 6. These two systems were designed to be compatible with any launch vehicle to allow for swapping launches with ease.

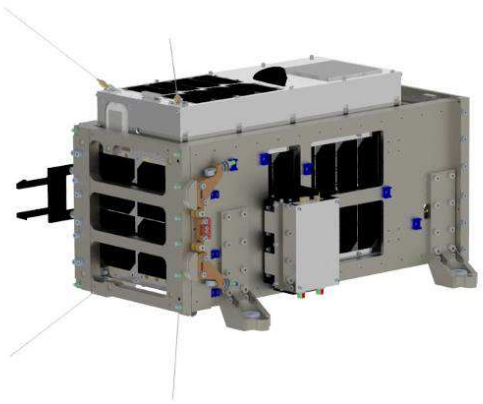

Figure 6: GHGSat-C1 in XPOD Delta Separation System

Phase 1 Demonstration: GHGSat-D

The GHGSat-D platform was based off the baseline NEMO bus. For ACS, it included five sun sensors, a rate sensor, a magnetometer, three orthogonal reaction wheels, three magnetorquers, a GPS and a star tracker. The radio system included a UHF uplink using four monopole antennas and S-band downlink using patch antennas. Command and data handling was performed using on-board computers cross-connected to all other hardware. The power architecture used SFL's modular power system (MPS) to distribute the 28 W generated from the body mounted triple-junction solar arrays and a 12 V Lithium-ion battery. Figure 7 shows GHGSat-D assembled.

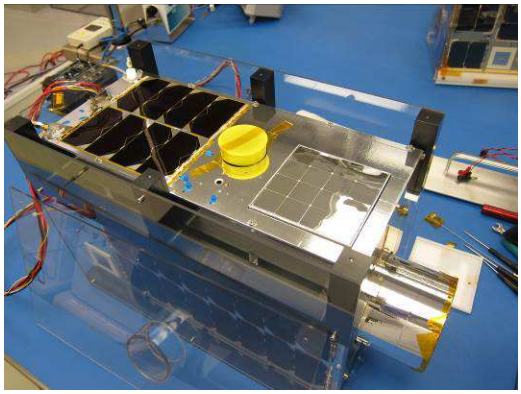

Figure 7: GHGSat-D in its Lunch Box

The primary payload was a Fabry-Perot imaging spectrometer operating at wavelengths between 1600-1700 nm, short-wave infrared (SWIR), and had a spectral resolution on the order of 0.1 nm. In addition, the design had three lens groups as well as beam folding mirrors which allowed the telescope to be scaled down to fit within the GHGSat-D bus. This payload was controlled by a Q7 processor provided by

Xiphos Systems Corporation. The secondary payload was a clouds and aerosols (C&A) sensor used to measure interference from clouds and aerosols in the field of view of the main payload. This sensor had a spectral range of 400-1000 nm with a 1.9 nm spectral resolution. Figure 8 shows a photograph of the completed GHGSat-D payload.

Figure 8: GHGSat-D Payload

The spacecraft launched into a 512 km. 9:30 LTDN sun synchronous orbit on June 22, 2016. To this day, it has been operating successfully on-orbit. This has allowed GHGSat to acquire a massive dataset to assess the performance of the payload and the review the quality of data that it produces.

Figure 9: GHGSat-D on PSLV C34[4]

Phase 2 Enhanced NEMO Platform: GHGSat-C1/C2

The overarching design of GHGSat-C1 is a clone of GHGSat-D with enhancements to both the bus side and payload side based on the lessons learned from the GHGSat-D development, its years on orbit and the technology advancement since its inception. These enhancements fall into three main categories: SFL upgrades, additional payloads, and main payload improvements. GHGSat-C2 is intended to be a clone of GHGSat-C1 with additional primary payload adjustments.

SFL Bus Upgrades

The mechanical design of GHGSat-C1 is largely identical to its predecessor. Minor modifications were made but this was done to support the additional payloads and the SFL upgrades. The exterior layout is shown in Figure 10.

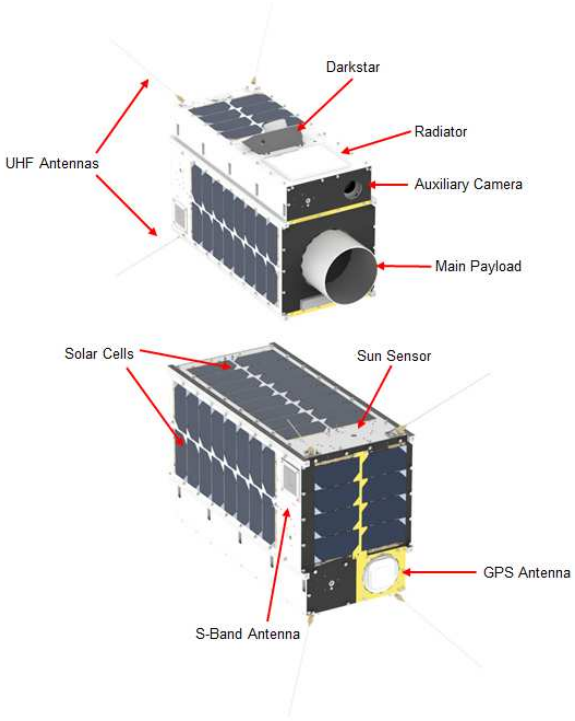

Figure 10: GHGSat-C1/C2 Exterior Layout

The uplink radio remains the same as GHGSat-D however the S-band transmitter has been replaced with a newer, higher power version. This allows for increased transmit gain to increase data transfer from the spacecraft to the ground. EMI gasketing was added to the primary spacecraft structure to improve uplink sensitivity of the bus. Gasketing was also added to the UHF enclosure itself. This resulted in the largest mechanical change from GHGSat-D as the interfaces between panels and trays needed to be adjusted to accommodate the gasket. Figure 11 shows the examples of how the gasketing was implemented.

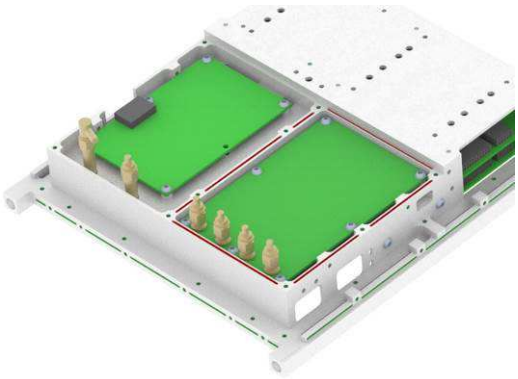

Figure 11: EMI Gaskets for UHF Receiver (Shown in Red) and Panel-Tray (Shown in Green)

For redundancy, a fourth reaction wheel was added. It is set in the standard skew configuration, as shown in Figure 12, such that it has control authority in the three principal spacecraft axes which allows it to replace any wheel. Although nominally designated a cold spare for backup, it can be used to avoid zero-crossings during imaging. This is of potentially great benefit since pointing accuracy is affected at low wheel speeds. In the standard three wheel orthogonal configuration, the control torque and wheel actuation is mapped one-to-one. However, the addition of the fourth wheel allows control torque to be distributed to the wheels in a variety of ways to allow the wheels to reach the desired speeds while avoiding the disturbances caused by zero-crossings.

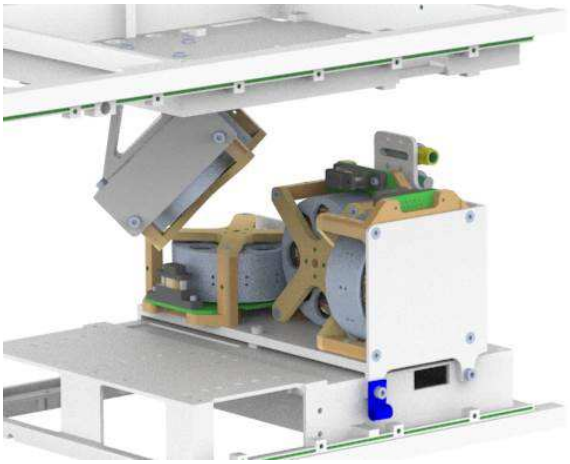

Figure 12: Reaction Wheels in Skew Configuration

To assist with ensuring positive power margins while the spacecraft is in Safehold, a permanent magnet has been added. During normal operations, the payload face of the spacecraft should never face the Sun; solar cells were left off the face to allow for a larger payload aperture. However, if the spacecraft did become locked in an attitude where the payload face is pointed at the Sun, it would become power negative until its attitude could be changed. The added magnet has been sized such that the dipole produced by the spacecraft will induce a magnetic torque when it interacts with the local magnetic field. This eliminates the possibility of entering the sun stare attitude. Figure 13 shows the average spacecraft power generation during Safehold mode for two different dipole values over several orbits.

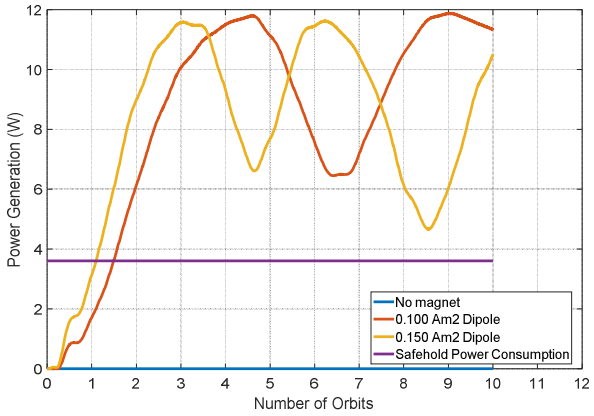

Figure 13: Average Satellite Power Generation for Various Dipoles along the Y-axis in a Payload face Sun Stare Attitude

Additional Payloads

GHGSat-C1 has two additional payloads compared to its predecessor. The first is Sinclair Interplanetary's Darkstar which is an experimental optical downlink and the second is Xiphos Systems Corporation's next generation Q8 processor.

During standard operations, GHGSat-D makes contact with two Earth stations located at SFL in Toronto, Canada and Inuvik, Canada with current monthly data volumes in excess of 7 GB. GHGSat-C1 will be the first spacecraft to fly Darkstar. This unit is a combined star tracker and optical downlink. See Figure 14 for the Darkstar internal layout. The optical downlink is intended to be able to downlink at rates up to 1 Gbps and once commissioned, will be used to boost the downlink capability of the spacecraft. The optical downlink uses a laser of wavelength 785 nm and is set transmit at an angle of 125˚ from the boresight of the star tracker. This unit is ~400 g and measures 100 x 68 x 68 mm.

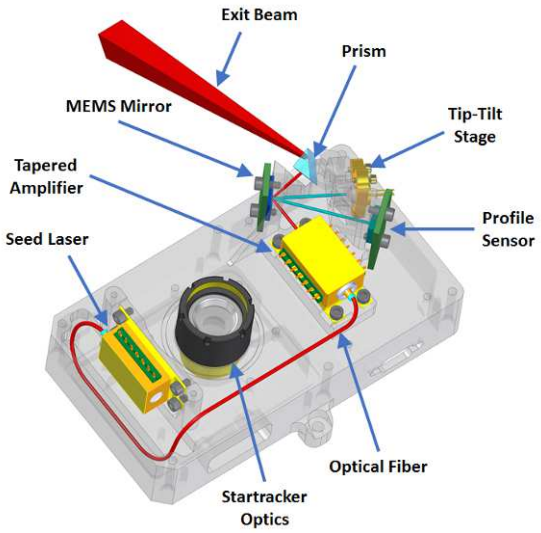

Figure 14: Darkstar Internal Layout[5]

The Q8 processor is the next generation of the Q7 processor that currently is used by the main payload and was added to GHGSat-C1 to gain flight heritage. It will serve as an interface between Darkstar and the primary payload to allow high speed data transfer via Ethernet. This will allow payload data stored on the Q7 to be transferred quickly to Darkstar for downlink to the ground. While the baseline remains to transmit payload data using S-band, the large data sets produced by the primary payload will be used for testing and characterization of the optical downlink

The addition of these two payloads did add some challenges for the accommodation and assembly of the spacecraft. The larger size of Darkstar versus the stand-alone star tracker required larger cutouts in the panel and the rearrangement of some internal components which consequently also required the wiring harness to be updated. To minimize the cutout and increase the ease of assembly, a split panel design was implemented as seen in Figure 15. A new bracket also had to be designed to give Darkstar adequate line-of-sight to the ground station while simultaneously ensuring sufficient exclusion angles between the star tracker and celestial bodies during operations.

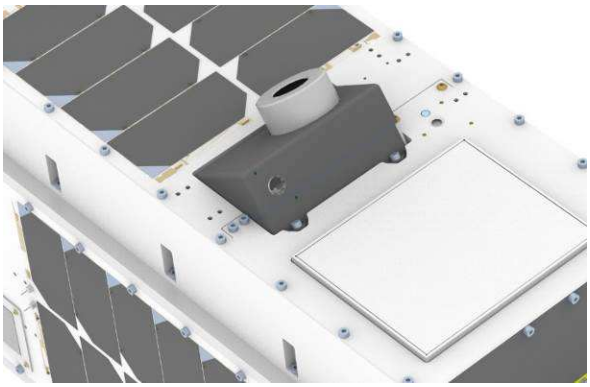

Figure 15: Split Panel Design to Accommodate Darkstar

The addition of the Q8 also introduced some challenges due to frequency conflicts between other spacecraft hardware caused by its high-speed data transfer. This necessitated an enclosure and cable shielding around the high speed data lines from the primary payload through the Q8 to Darkstar. The design of this enclosure proved challenging due to the extremely tight clearances with other hardware especially the reaction wheels. An example of the enclosure is shown in Figure 16.

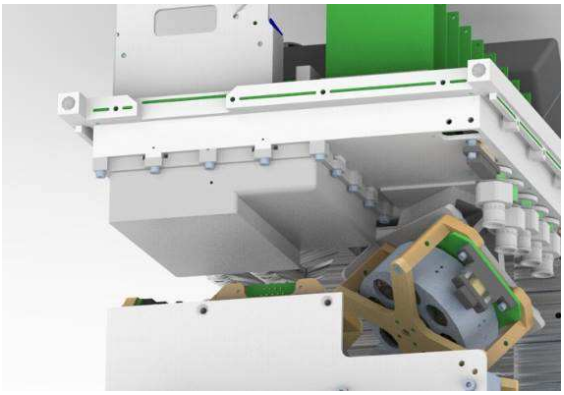

Figure 16: Q8 Processor Enclosure

Main Payload Improvements

Based on the data collected by GHGSat-D, several upgrades to the primary payload were commissioned to improve performance and resilience. These upgrades serve to mitigate ghosting, stray light and radiation effects that have been observed during operation. Ghosting is the zoomed, reflected, rotated or translated copies of the intended image. The primary method that ghosting was addressed was though optical coatings. While the GHGSat-D payload had anti-reflective coatings, these were both updated and added to more surfaces along the optical path. Further, the passband was narrowed to focus solely on methane. This is unlike the GHGSat-D payload which restricted the spectral

passband to 1600-1700 nm wavelengths to allow both methane and carbon dioxide. Stray light is the extra light that the payload sensor unintentionally observes during operation. From the GHGSat-D data, it was determined that as much as 5% stray light was getting to the sensor with the majority being from off-axis incident light. Several elements of the optical system were re-evaluated and redesigned to decrease stray light. The final issue that the new payload attempts to resolve is detector degradation due to radiation. The new payload has extra radiation shielding added around the detector to help increase its lifetime. Figure 17 shows the completed GHGSat-C1 payload.

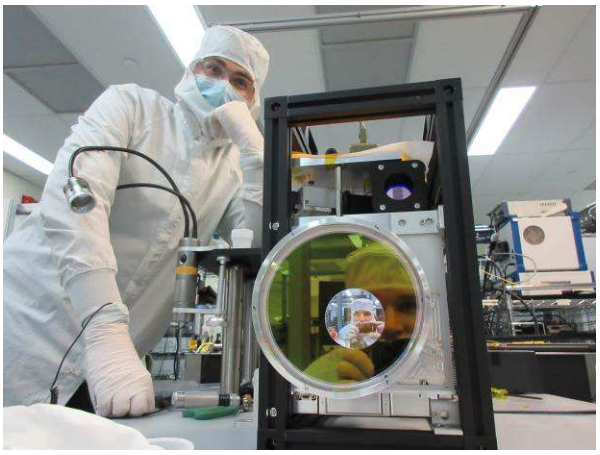

Figure 17: GHGSat-C1 Payload

The final upgrade was to replace the C&A camera secondary payload as it was determined to not have any significant contribution to the mission. This payload was replaced with an auxiliary camera that operates in the visible spectrum. This payload, through its higher resolution images, will allow for improved image alignment and georeferencing of the images taken by the main payload.

CURRENT STATUS AND FUTURE PLANS

GHGSat-C1/GHGSat-C2 will further GHGSat's goal of worldwide monitoring of GHG emissions and enable more frequent tracking of target sites. They serve as a precursor to a full constellation allowing continued refinement of the payload. GHGSat-C1 is assembled and currently undergoing final system level testing. Figure 18 shows the fully assembled GHGSat-C1 in the SFL EMC chamber. It is on track for launch in September 2019 into a 515 km 10:30 LTDN sun synchronous orbit. GHGSat-C2 is beginning construction with the goal of launching in the first half of 2020. GHGSat-C1 and GHGSat-C2 are the first two satellites in a planned constellation of 10 GHG monitoring satellites.

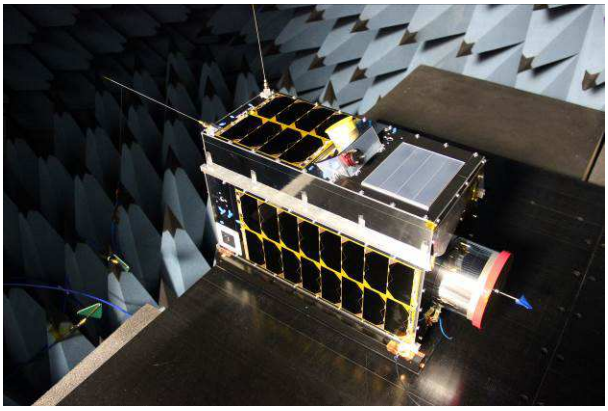

Figure 18: Fully Assembled GHGSat-C1 Satellite in the SFL EMC Chamber

CONCLUSION

The enhancements to the spacecraft serve to increase the reliability and performance of the system, increasing the data quality that can be produced. Additional technologies will be tested that will further benefit the future constellation to increase the amount of data that can be transferred from the spacecraft. GHGSat-C1 and GHGSat-C2 serve as the next step on the road to a worldwide GHG monitoring system.

Figure 19: Artists Rendition of GHGSat Constellation

Acknowledgments

The authors would like to acknowledge the support of the Government of Canada, through Sustainable Development Technology Canada and the Industrial Research Assistance Program, Emissions Reduction Alberta, Ontario Centres of Excellence, LOOKNorth, and the Canadian Space Agency. The authors would also like to thank our colleagues at SFL, GHGSat, MPB Communications, Xiphos, and Sinclair Interplanetary for their hard work and contributions to these missions.

References

1. Government of Canada, Canada's 7th National Communication and 3rd Biennial Report.

Gatineau, QC: Environment and Climate Change Canada, 2017.

2. J. Sheng et al., "2010-2016 methane trends over Canada, the United States, and Mexico observed by the GOSAT satellite: contributions from different source sectors," *Atmospheric Chemistry and Physics*, vol. 18, pp. 12257-12267, 2018.

3. *Lom Pangar Dam, Cameroon - April 20th, 2017 GHGSat-D excess CH4 column measurement* [Photograph found in GHGSat Inc, Montreal]. (2017, August 18). Retrieved June 7, 2019, from https://www.ghgsat.com/case-studies/case-study-3/ (Originally photographed 2017, April 20)

4. *All the 20 Spacecrafts integrated with PSLV-C34 - two halves of the heat shield are seen* [Photograph found in Department of Space Indian Research Organization, India]. (n.d.). Retrieved June 7, 2019, from https://www.isro.gov.in/pslv-c34-cartosat-2-series-satellite/pslv-c34-gallery?page=1

5. D. Sinclair and K. Riesing, "The Rainbow Connection – Why Now is the Time for Smallsat Optical Downlinks," in Proc. 31st Annual AIAA/USU Conference on Small Satellites, 2017.